ACS OMEGA

http://pubs.acs.org/journal/acsodf

Article

Effects of Molecular Properties on Adsorption of Six-Carbon VOCs by Activated Carbon in a Fixed Adsorber

Show-Chu Huang, Tsair-Wang Chung, and Hung-Ta Wu*

Cite This: *ACS Omega* 2021, 6, 5825−5835

Read Online

ACCESS | Metrics & More | Article Recommendations

ABSTRACT: Gravimetric adsorption equipment with a microbalance was used to measure the adsorption of volatile organic compounds (VOCs) by activated carbon from 288 to 313 K. VOCs [*n*-hexane, cyclohexane, 1-hexene, 2-methylpentane, 3-methylpentane, 2,2-dimethylbutane, acetone, butanone, and 2-pentanone (Pentan-2-one)] were used as adsorbates in the adsorption system. Considering the geometric barrier, the critical diameter, and the boiling point, the adsorption capacities for six-carbon (C_6) alkane isomers decrease in the order of *n*-hexane, 3-methylpentane, and 2-methylpentane. The adsorbates, including nonpolar or weakly polar substances, and substances with smaller geometric obstacles and smaller molecular weights, were more easily adsorbed by the activated carbon. However, the dipole−dipole interactive force at higher pressures resulted in a higher adsorption capacity for 1-hexene than for *n*-hexane. Both polarity and molecular size should be considered in the analysis of the adsorption of ketones by activated carbon. The adsorption equilibrium constants decreased with increases in temperature because a higher temperature was unfavorable for adsorption. The results for the Toth adsorption isotherm model fitted by the adsorption data showed that the experimental data and the Toth adsorption isotherm model were consistent with each other, as evidenced by the low deviation between the experimental data and those from the fitted model.

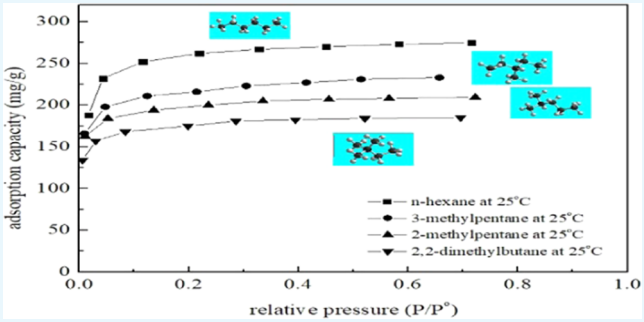

1. INTRODUCTION

The sources of VOCs in the atmosphere are complex, and they can be classified into stationary pollutants and mobile pollutants.[1] For example, gas stations, semiconductor plants, and petrochemical plants are stationary pollutants, and vehicles using fossil fuels are mobile pollutants. The largest emission of VOCs arises from the use of organic solvents, which are widely used in various industries because of their multiple physicochemical properties. Human health and the environment can be destroyed by many VOCs; therefore, removal of VOCs from the air is necessary. The methods for removing VOCs can be divided into two categories: nondestructive and destructive methods.[2] When VOCs are treated using nondestructive methods, such as adsorption, absorption, and condensation, the recycled VOCs can be reused. Destructive methods, such as incineration and biological treatment methods, decompose VOCs into water and carbon dioxide. The adsorption method, which is a removal technology for purifying air, is not only applicable to a wide range of concentrations but also highly effective. Thus, this method is adopted widely in industries to remove gaseous pollutants.

The VOCs used in this study included *n*-hexane, 1-hexene, cyclohexane, 2-methylpentane, 3-methylpentane, 2,2-dimethylbutane, acetone, butanone, and 2-pentanone. To examine the effect of molecular polarity on the adsorption capacity, the adsorption of ketones and *n*-hexane on activated carbon were compared. The VOCs with different molecular shapes selected in this study are often released into indoor environments. *n*-Hexane can be found in lacquers, glues, and glue thinner, and it is applied in industrial processes. Polyneuropathy can be induced by *n*-hexane; the actual pathogenesis was derived by Huang.[3] Therefore, *n*-hexane and other VOCs were monitored by Pegas et al.[4] to verify indoor/outdoor air quality, and the results showed that environments with closed windows had higher indoor levels of VOCs released by building materials and consumer products. Although 1-hexene can cause headaches, dizziness, nausea, and difficulty in breathing in humans, it can also be used to produce important chemical materials. For example, catalytic cracking was used by Nawaz et al.[5] to produce propylene from 1-hexene in the presence of a 30% SAPO-34 catalyst. Rösch et al.[6] described that glue emissions and decorations could be sources of cyclohexane in

Received: December 24, 2020
Accepted: February 10, 2021
Published: February 18, 2021

https://dx.doi.org/10.1021/acsomega.0c06260
ACS Omega 2021, 6, 5825−5835

Table 1. Recent Studies Related to VOC Removal in the Fixed-Bed Adsorber

focus	adsorbent	adsorbate	authors
performance improvement	fluidized activated carbon bed	styrene	Mofidi et al.[19]
performance improvement	granular activated carbon	toluene	Dehdashti et al.[20]
performance improvement	activated carbon	toluene	Pak and Jeon[21]
performance improvement	activated carbon fiber cloth	MEK	Sullivan et al.[22]
performance improvement, modeling	activated carbon	chloromethane	Lemus et al.[23]
modeling and performance testing	activated carbon	chloroform and carbon tetrachloride	Kalender and Akosman[24]
modeling and performance testing	activated carbon	toluene, benzene, and xylene	Das et al.[25]
modeling	coolant and activated carbon	dimethyl chloride and toluene	Gupta and Verma[26]
modeling	activated carbon	*n*-butanol, *n*-butylacetate, 2-heptanone, 2-butoxyethanol, *n*-decane, indan, 2,2-dimethylpropybenzene, and 1,2,4-trimethylbenzene	Tefera et al.[27]
performance testing	activated carbons	siloxanes and VOCs	Cabrera-Codony et al.[28]
performance testing	glucose-adsorbent	ethane/ethylene	Ma et al.[29]
performance testing	xGnP, zeolite, and perlite	total VOCs and formaldehyde	Chang et al.[30]
performance testing	activated carbon fiber, pp, pp, and activated carbon	formaldehyde, toluene, and benzene	Moon et al.[31]
performance testing and preparation of absorbent	almond shell-based activated carbon	toluene and toluene/water vapor	De Yuso et al.[32]
preparation of absorbent	activated carbon	carbon tetrachloride, benzene, ether, and n-pentane	Anuradha et al.[33]
preparation of absorbent	MWCNTs	benzene and toluene	Pourfayaz et al.[34]
modification of absorbent	ZSM-5 prepared with and without an organic template	benzene, toluene, ethylbenzene, and xylene	Aziz et al.[35]
modification of absorbent	organic substance: modified titanate nanotubes (TNTs)	toluene, ethylbenzene, 1-1-2 trichloroethane, and tetrachloroethane	Wang et al.[36]
modification of adsorbent	modified clinoptilolote natural zeolite	acetone	Aghababaei[37]
analysis of physicochemical properties	activated carbon fiber	methanol, ethanol, propan-1-ol, butan-1-ol, n-octane, and *n*-nonane	Nwali[38]

indoor environments. The ratios of the concentrations of VOCs indoor and outdoor were measured by Norbäck et al.,[7] and the results showed that cyclohexane concentrations were higher in indoor environments than in outdoor environments. Using chromatography-mass spectrometry, Gallego et al.[8] and Araizaga et al.[9] demonstrated that 2-methylpentane was found indoors and was emitted by light-duty vehicles. An adsorption bed packed with zeolite silicalite was used by Schuring et al.[10] to separate a mixture of *n*-hexane/2-methylpentane. Araizaga et al.[9] and Graham et al.[11] confirmed that emissions from vehicles contributed to the accumulation of 3-methylpentane in indoor environments. In addition, Han et al.[12] showed that 3-methylpentane could be a byproduct of oxidizing benzene by a TiO_2 photocatalyst. Since the difference between these VOCs found in indoor environments is in the molecular structure, they were selected as target VOCs to be adsorbed in this study. Akihama et al.[13] and Liu et al.[14] reported that 2,2-dimethylbutane always resulted from environments with higher temperatures. In humans, the symptoms of exposure to 2,2-dimethylbutane include headache, dermatitis, and damage to the kidneys and bladder. Since dehydrogenation of 2,2-dimethylbutane can be carried out in the presence of a catalyst, alumina-supported platinum−rhenium and iridium were used as catalysts by Garland et al.[15] and Vogelzang and Ponec,[16] respectively, to treat 2,2-dimethylbutane. The dibranched 2,2-dimethylbutane was not only adsorbed by zeolite[17] but also separated from the isomer hexane by silicalite-1.[18] Such collected 2,2-dimethylbutane can be reused for enhancing gasoline octane numbers.

As shown in Table 1, studies related to removing VOCs have focused on various aspects, including performance improvement, modeling, performance testing, preparation of adsorbent, modification of adsorbent, and analysis of physicochemical properties. For example, activated carbon was used by Mofidi et al.,[19] Dehdashti et al.,[20] and Pak and Jeon[21] to discuss its adsorption capacities for styrene and toluene. To obtain more knowledge on the behaviors of the breakthrough curve, the Yoon and Nelson model was applied by Lemus et al.[23] and Kalender and Akosman[24] to predict the breakthrough curves for removing chlorinated VOCs. A mathematical model involving the nonequilibrium approach, individual kinetic rate expressions, the effects of pore diffusion, and gas−fiber mass transfer resistance was developed by Das et al.[25] to predict the breakthrough characteristics for adsorbing VOCs. Similarly, a mathematical model based on cryogenic condensation and adsorption methods was developed by Gupta and Verna[26] to predict the removal amount for adsorption of VOCs in the air. In addition, a two-dimensional mathematical model combining an isotherm equation with a dynamic adsorption model was derived by Tefera et al.[27] to study competitive adsorption of *n*-component mixtures in a fixed-bed adsorber. The adsorbents, including granular activated carbon, glucose- and almond shell-based adsorbents, activated carbon fibers, and zeolite, were used to remove VOCs to investigate the effects of operating variables on the adsorption capacity.[28−32] For adsorbents, the effects of the preparation variables of the adsorbents on the surface properties and the amounts of VOCs removed by the prepared adsorbent were reported,[32−34] and some studies[35−37] reported that the removal amount of VOCs could be increased by the modified adsorbent. However, discussions of the relationship between adsorption performance and physicochemical properties in the literature have been limited. One study reported on the adsorption of VOCs by wood-based activated carbon,[38] and the results showed that the performance was affected by the functional groups and the activation energy. The current study

https://dx.doi.org/10.1021/acsomega.0c06260
ACS Omega 2021, 6, 5825−5835

differs from the above one, focusing on adsorbates having different structures. Since the studies discussing the relationships between adsorption performance and physicochemical properties are rare, the significance of this study was to remove adsorbates having different structures with a packed-bed adsorber and then to determine how the adsorption capacity is affected by physicochemical properties, such as critical diameter, boiling point, molecular structure, and polarity.

The internal surface area of activated carbon is larger than the external surface area; the former is the key factor that determines the amount of VOCs adsorbed by the porous adsorbent. In general, the specific surface area of the activated carbon ranges from 500 to 1500 m^2/g, and its porosity is on the scale of nanometers. The design of adsorption equipment requires equilibrium data, which can be acquired from adsorption experiments.[2] One type of equilibrium data is the adsorption isotherm, which is often referred to by adsorber designers. The amount of adsorbent needed in an adsorber may be dependent on the adsorption isotherm, and an effective adsorbent can be selected according to the adsorption isotherm and the breakthrough curve. In this study, the equilibrium isotherm data were obtained with a static gravimetric system wherein the amount of VOCs adsorbed onto a solid surface was measured by a microbalance, and the adsorption capacity was obtained under controlled pressures and temperatures.

Heterogeneous adsorption occurs when gaseous VOCs are adsorbed by solid activated carbon. Since the Toth adsorption isotherm model is suitable for modeling a heterogeneous reaction or process, it was used for regression of the adsorption data in this study. When the adsorption exponent approaches 1, the Toth adsorption isotherm model can be simplified to the Langmuir adsorption model. However, when the concentration of the adsorbate approaches zero, the Toth adsorption model can be translated into Henry's law. The adsorption capacities or uptakes were obtained under controlled pressures, and then the uptakes were regressed by the Toth adsorption isotherm model to analyze the mechanisms of different structural VOCs being adsorbed by activated carbon in this study.

2. EXPERIMENTAL SECTION

2.1. Sorbents. The commercial granular activated carbon used in this study was supplied by China Activated Carbon Industries Co. The surface properties were measured with a BET sorptometer (Micromeritics ASAP 2000) and are shown in Table 2. The adsorbent was degassed at 473 ± 0.1 K under vacuum for 24 h before adsorption measurements of nitrogen were carried out at 77 ± 0.1 K. The specific surface area, pore volume, and average pore diameter were measured and calculated by the BET method. The surface area was 919 m^2, and most pore sizes were in the range of micropore and mesopore. The average pore diameter was 1.43 nm.

Table 2. Surface Properties of Activated Carbon[a]

property	value
BET surface area, A (m^2/g)	919
V_{total} (cm^3/g)	0.46
V_{meso} (cm^3/g)	0.21
V_{micro} (cm^3/g)	0.24
V_{macro} (cm^3/g)	0.09
pore diameter, D (nm)	1.43

[a]Standard uncertainties are $u(T)$ = 0.1 K, $u(P)$ = 0.026 kPa, $U(A)$ = 4 m^2/g, $U(V_{total})$ = 0.0033 cm^3/g^{-1}, $U(V_{meso})$ = 0.0029 cm^3/g^{-1}, $U(V_{micro})$ = 0.0038 cm^3/g, $U(V_{macro})$ = 0.0044 cm^3/g, and $U(D)$ = 0.0036 nm.

2.2. Chemicals. Six-carbon VOCs (*n*-hexane, 1-hexene, cyclohexane, 2-methylpentane, 3-methylpentane, 2,2-dimethylbutane) were used in this study. To compare the effect of the length of the carbon chain on adsorption behaviors, adsorptions of acetone, butanone, and 2-pentanone were also employed in this study. These VOCs, which are released by gasoline and solvents commonly used in industries, may appear as pollutant organic compounds in daily life, and they can cause harm to the human body and the environment. The VOCs mentioned above were used as adsorbates to be adsorbed by activated carbon, and the adsorption isotherms were acquired to examine the adsorption behaviors. All chemicals were of reagent grade, and their physical and chemical properties are provided in Table 3.

2.3. Adsorption System and Procedure. Figure 1 shows the adsorption system used in this study, and the glass valves were used in the system. The change in mass during the adsorption process was measured with an electronic microbalance (Cahn C-33). The uncertainty of the microbalance is ± 0.1 μg. The system was maintained at pressures ranging from 1.333×10^2 Pa (1 mm Hg) to 32.664×10^3 Pa (245 mm Hg), as measured with a pressure gauge (Cole Parmer U-68700, uncertainty = ±0.1333 Pa).

The step-by-step procedure by which the adsorption capacity of VOCs on the adsorbent was measured by gravimetric adsorption is provided below:

(1) Briefly, 50 mg of a granular adsorbent was placed on a pan of the electric microbalance (Cahn C-33) after the adsorbent was regenerated in a vacuum dryer at 373 K for 24 h.
(2) The liquid VOC adsorbate was placed in glass bottles, as shown in Figure 1. The degassing procedure was repeated at least three times.
(3) V_1, V_2, V_3, and V_4 were opened and V_5 and V_6 were closed to allow for the vapor of the liquid adsorbate (VOC) to enter the adsorption system.
(4) When the preset pressure was reached, V_3, V_4, V_5, and V_6 were closed.
(5) The amounts of the adsorbent and adsorbate and the pressure of the adsorption system were recorded when the weight displayed on the panel was unchanged.
(6) The pressure of the VOCs in the adsorption system was changed.
(7) The amounts of the adsorbent and sorbate and the pressure of the adsorption system were recorded.
(8) Steps (6) and (7) were repeated until a saturated pressure was attained.

3. RESULTS AND DISCUSSION

3.1. Adsorption Capacity. The adsorption data from Zhao et al.[43] and Ramirez et al.[44] were used to compare adsorption tests in this study, and the surface characteristics of the adsorbents for these studies are listed in Table 4. Since the surface characteristics of the activated carbon and the operating conditions in this study were similar to those in Zhao et al.,[43] the trends of the adsorption isotherm were similar, as shown in Figure 2. The surface area of the activated carbon used by Ramirez et al.[44] was larger than those used by

https://dx.doi.org/10.1021/acsomega.0c06260
ACS Omega 2021, 6, 5825−5835

Table 3. CAS Registry Number, Suppliers, Mass Fraction Purity, and Physical and Chemical Properties of the Chemicals[a]

adsorbate	*n*-hexane	cyclohexane	1-hexene	2-methyl-pentane	3-methyl-pentane	2,2-dimethyl-butane	acetone	butanone	2-pentanone
CAS Reg. No.	110-54-3	110-82-7	592-41-6	107-83-5	96-14-0	75-83-2	67-64-1	78-93-3	107-87-9
supplier	Tedia company	Tedia company	Acros Organics	Lancaster Synthesis	Lancaster Synthesis	Lancaster Synthesis	Leda Chemcial	Tedia company	Tedia company
mass fraction	99	99.5	97	98	97	99	99.5	99.5	99.47
molecular formula	C_6H_{14}	C_6H_{12}	C_6H_{12}	C_6H_{14}	C_6H_{14}	C_6H_{14}	C_3H_6O	C_4H_8O	$C_5H_{10}O$
molecular weight (g/mol)	86.17[42]	84.16[42]	84.16[42]	86.17[42]	86.18[41]	86.17[42]	58.08[42]	72.11[42]	86.13[42]
boiling point (K)	341.8[42]	353.8[42]	336.6[39]	333.4[42]	336.2[41]	322.7[42]	329.3[42]	352.7[42]	375.4[42]
dipole moment (D)	0[39]	0.3[39]	0.4[39]	0.1[41]			2.9[39]	3.3[39]	2.5[39]
L-J potential constant (Å)	5.91[49]	6.09[49]	5.81[50]	5.75[50]	5.83[50]	5.75[50]	4.70[51]	5.04[51]	5.37[51]
kinetic diameter (nm)	4.54[52]	5.70[40]	6.00[53]	6.10[40]	6.10[40]	6.10[40]	4.40[54]	5.25[54]	5.20[55]
critical diameter (nm)	4.90[56]	6.90[40]		5.40[40]	5.40[40]	6.30[40]			
critical temperature[39] (K)	507.5	553.5	504.0	497.5	504.4	488.7	508.1	536.8	561.6
critical pressure[39] (kPa)	2968.82	4073.27	3171.47	3009.35	3120.81	3080.28	4701.48	4154.33	3890.88
vapor pressure[42] at 288 K (kPa)	12.80	8.13	15.87	18.27	17.07	29.06	19.60	7.47	2.67
298 K (kPa)	20.13	13.07	24.66	28.00	25.46	44.26	30.53	12.27	4.67
308 K (kPa)	43.86	20.13	37.06	41.73	39.46	61.86	46.26	19.20	7.74
318 K (kPa)	44.93	30.13	53.86	60.39	55.33	89.33	67.86	29.33	12.40

[a]42@1997 McGraw-Hill;41@1999 Prentice Hall;39@1977 McGraw-Hill;49@1979 Springer;50@1967 Royal Society of Chemistry;51@1994 Elsevier;52@2004 Elsevier;40@1995 American Chemical Society;53@2003 Elsevier;54@2012 Elsevier;55@2010 Wiley-Blackwell;56@2015 Sciencedomain international.

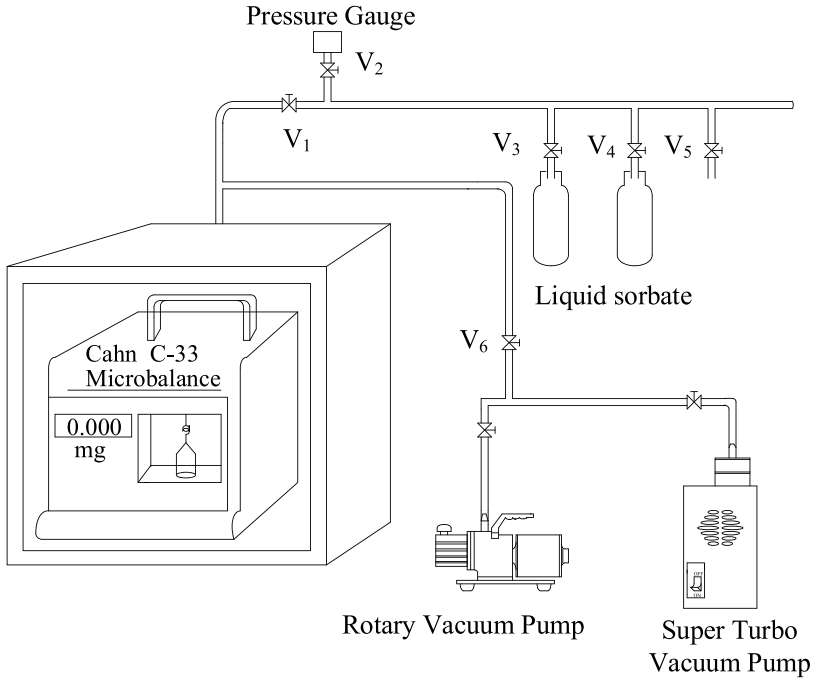

Figure 1. Gravimetric adsorption system of this study (static gravimetric method).

Table 4. Surface Characteristic Comparison between the Literature Study and This Study[a]

	Zhao et al.[43]	Ramirez et al.[44]	This study
adsorbate	*n*-hexane	*n*-hexane	*n*-hexane
adsorbent	Activated carbon	Activated carbon	Activated carbon
BET surface area, A (m^2/g)	923	965	919
V_{total} (cm^3/g)	0.46	0.615	0.46
pore diameter, D (nm)		2.55	1.43
temperature, T (K)	295	293 and 303	298

[a]Standard uncertainties are $u(T)$ = 0.1 K, $u(P)$ = 0.026 kPa, $U(A)$ = 4 m^2/g, $U(V_{total})$ = 0.0033 cm^3/g, and $U(D)$ = 0.0036 nm for this study.

https://dx.doi.org/10.1021/acsomega.0c06260
ACS Omega 2021, 6, 5825−5835

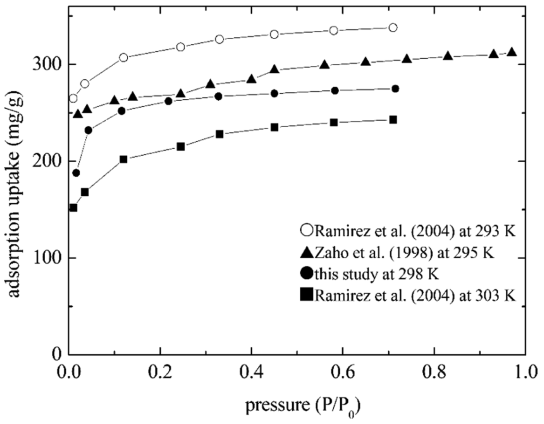

Figure 2. Comparing the adsorption data in this study with the literature study. Standard uncertainties are $u(T)$ = 0.1 K and $u(P)$ = 0.026 kPa and the mean standard uncertainty is 1.13 mg/g for this study.

Zhao et al.[43] and this study. Furthermore, the adsorption capacity is better for the lower temperature. Therefore, the adsorption capacity conducted by Ramirez et al.[44] at 293 K was higher than that in this study, and the adsorption capacity at 303 K was lower than that in this study. Since a similar trend among the literature data and this study was observed, the adsorption system established in this study was reasonable.

The adsorption uptakes by activated carbon of nine VOCs (*n*-hexane, 1-hexene, cyclohexane, 2-methylpentane, 3-methylpentane, 2,2-dimethylbutane, acetone, butanone, and 2-pentanone) were measured, and the adsorption isotherms were also plotted to examine the effects of physicochemical properties on adsorption behaviors. Commercial activated carbon, which is easily available and cheap, has stable surface properties; therefore, it was used to adsorb VOCs commonly found in the environment. The important characteristics of VOCs include molecular structure, boiling point, bonding type, polarity, and molecular weight. Since the molecular weights of *n*-hexane and cyclohexane are similar, the adsorption data for them were used to examine the effects of the molecular structure on adsorption capacities. Adsorptions of *n*-hexane and 1-hexene were compared to analyze how the adsorption capacity was affected by the bonding type. Since the polarity of 2-pentanone is larger than that of *n*-hexane, adsorption tests of *n*-hexane and 2-pentanone were compared to analyze how the adsorption capacity is affected by polarity. Finally, to examine the effects of molecular weight on the adsorption capacity, acetone, butanone, and 2-pentanone were adsorbed by the activated carbon.

3.2. Adsorption Isotherms for *n*-Hexane and Its Isomers. Both alkanes and activated carbons are nonpolar or weak polar substances. When adsorption occurs in such a pair, the adsorption capacity may be dominated by the molecular size and the structure of the adsorbate. Therefore, information related to the molecular size and structure of the adsorbate would be helpful for analyzing the adsorption behaviors of the adsorbent and the adsorbate. Zhu et al.[45] described how the kinetic diameter and Lennard-Jones potential constant (L-J constant) could be used to assess if gas or vapor molecules easily diffuse into the pores of a material. However, this approach has been contradicted in some reports.[46−48] Therefore, the critical diameters of the adsorbates were considered to explain the adsorption phenomenon in this study. The molecular structures of the adsorbates selected in this study are shown in Figure 3. The

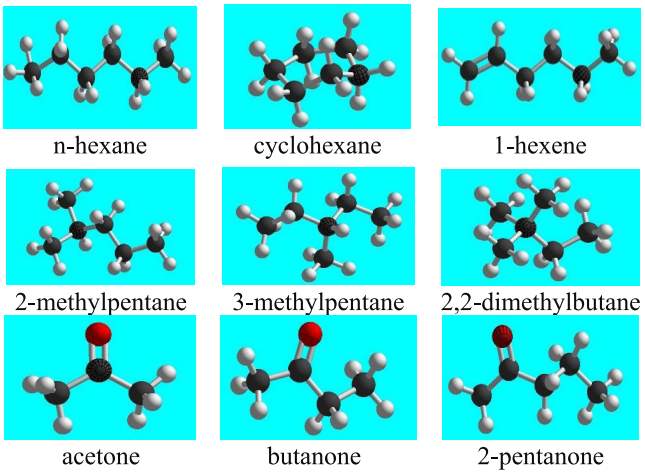

Figure 3. Molecular structures for the adsorbates used in this study.

physicochemical properties, such as dynamic diameter, L-J constant, and critical diameter, are listed in Table 3. The adsorption isotherms for *n*-hexane and its isomers adsorbed by the activated carbon at 298 K are shown in Figure 4. The

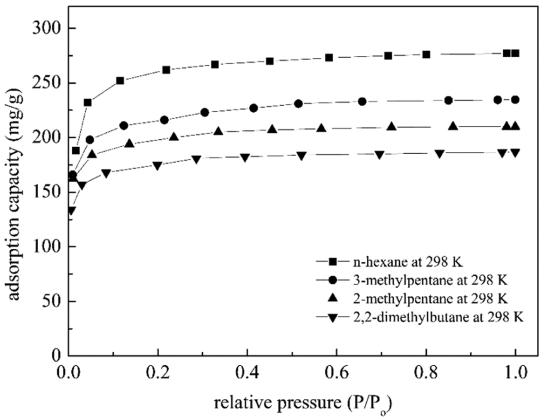

Figure 4. Adsorption capacities for *n*-hexane and its isomers. Standard uncertainties are $u(T)$ = 0.1 K and $u(P)$ = 0.026 kPa and the mean standard uncertainties are *n*-hexane = 1.13, 3-methylpentane = 1.40, 2-methylpentane = 1.56, and 2,2-dimethylbutane = 1.58.

adsorption capacities decreased in the order of *n*-hexane, 3-methylpentane, 2-methylpentane, and 2,2-dimethylbutane. This result was ascribed to the presence of a branch in the other alkanes; as a result, the steric obstacle was smaller for *n*-hexane. In addition, the critical diameters decreased in the order of 2,2-dimethylbutane, 2-methylpentane = 3-methylpentane, and *n*-hexane, which explained why *n*-hexane diffused into the pores of the activated carbon more easily than did the others. Although the branched chains are contained within the structures of 2-methylpentane, 3-methylpentane, and 2,2-dimethylbutane, the latter has two methyl branches. These branches make the steric obstacle larger for 2,2-dimethylbutane; therefore, it cannot enter the pores of activated carbon as easily as can 2-methylpentane and 3-methylpentane. This explains why its adsorption capacity was the lowest (Figure 4). Both 2-methylpentane and 3-methylpentane contain methyl

https://dx.doi.org/10.1021/acsomega.0c06260
ACS Omega 2021, 6, 5825−5835

branches, but the steric structure of 3-methylpentane is more symmetric than that of 2-methylpentane. In addition, the boiling point of 3-methylpentane is slightly higher than that of 2-methylpentane, which likely also contributed to the slightly larger adsorption capacity for 3-methylpentane.

3.3. Adsorption Isotherms for *n*-Hexane and Other C_6 VOCs. Both *n*-hexane and cyclohexane, which have six-carbon chains, are nonpolar or weak polar substances. Their molecular structures and critical diameters must be analyzed to determine the adsorption capacities of nonpolar activated carbon for such substances. The adsorption isotherms shown in Figure 4, represented by the symbols ■ and ●, are those for adsorbing *n*-hexane and cyclohexane on activated carbon, respectively. The adsorption capacity for *n*-hexane was larger than that for cyclohexane, which could be attributed to the fact that the geometric barrier for annular and nonplanar structures of cyclohexane was larger than the linear structure of *n*-hexane. In addition, the critical diameter of cyclohexane is larger than that of *n*-hexane, which slightly inhibits the diffusion of cyclohexane into the pores of activated carbon relative to that of *n*-hexane. Therefore, the adsorption capacity is larger for *n*-hexane than for cyclohexane.

The structural difference between *n*-hexane and 1-hexene is the double bond in the latter. The adsorption isotherms for *n*-hexane and 1-hexene are shown in Figure 5. The adsorption

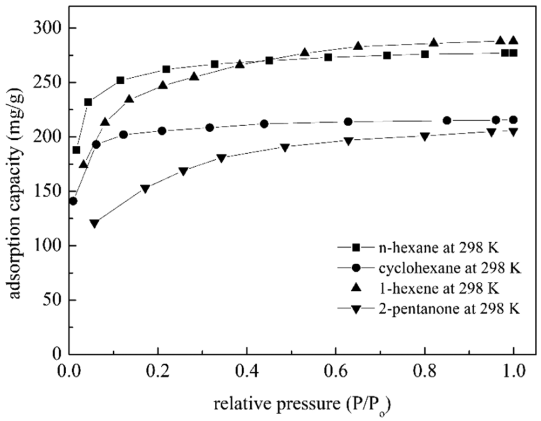

Figure 5. Adsorption capacities for *n*-hexane and different structure VOCs. Standard uncertainties are $u(T)$ = 0.1 K and $u(P)$ = 0.026 kPa and the mean standard uncertainties are *n*-hexane = 1.13, cyclohexane = 0.97, 1-hexene = 1.37, and 2-pentanone = 1.53.

capacity was larger for *n*-hexane than for 1-hexene at lower pressures, but the opposite was true at higher pressures. As shown in Table 3, *n*-hexane and 1-hexene are nonpolar and polar molecules, respectively. Therefore, in the adsorption of *n*-hexane and 1-hexene by activated carbon, all of the Van der Waals forces include dipole−dipole interaction, dipole-induced dipole interaction, and dispersion. Since substances of the same nature dissolve each other more easily, the adsorption capacity was larger for *n*-hexane than for 1-hexene at lower pressures. Therefore, at lower pressures, the effect of the dispersion between *n*-hexane and activated carbon was larger than the dipole-induced dipole interaction between 1-hexene and activated carbon.

Since more 1-hexene was adsorbed by the activated carbon at higher pressures than that at lower pressures, the effect of the dipole−dipole interaction between the adsorbed 1-hexene and the unadsorbed 1-hexene should be larger than the dispersion between the adsorbed *n*-hexane and the unadsorbed *n*-hexane. Furthermore, a methyl group with a double bond would be more elliptical and that with a single bond would be spherical. Zhu et al.[47] found that the smaller critical diameter resulted from olefins with an elliptical methyl group, which is why 1-hexene has a smaller critical diameter. The filling effect is better for 1-hexene than for *n*-hexane due to the smaller critical diameter. Due to the dipole−dipole interaction and the better filling effect, the adsorption capacity for 1-hexene was larger at higher pressures.

Due to the similar molecular weights but different polarities of *n*-hexane and 2-pentanone, they were used to examine the effect of polarity on the adsorption of an adsorbate by activated carbon. The adsorption capacity was larger for *n*-hexane than for 2-pentanone, as shown in Figure 5. This result also demonstrated that a nonpolar adsorbate is adsorbed on a nonpolar adsorbent more easily than is a polar adsorbate. Since the difference in adsorption capacities between *n*-hexane and 2-pentanone was significantly larger than that between *n*-hexane and 1-hexene, the cross-phenomenon of the adsorption isotherms did not occur in this case.

3.4. Adsorption Isotherms for Ketones. The major structural difference in acetone, butanone, and 2-pentanone is in the length of the carbon chain, which affects the molecular weight. Their molecular weights decrease in the order of 2-pentanone, butanone, and acetone. In addition, all have higher polarity, though their polarities decrease in the order of butanone, acetone, and 2-pentanone. The adsorption isotherms for adsorption of acetone, butanone, and 2-pentanone by activated carbon are shown in Figure 6, and the trend of the

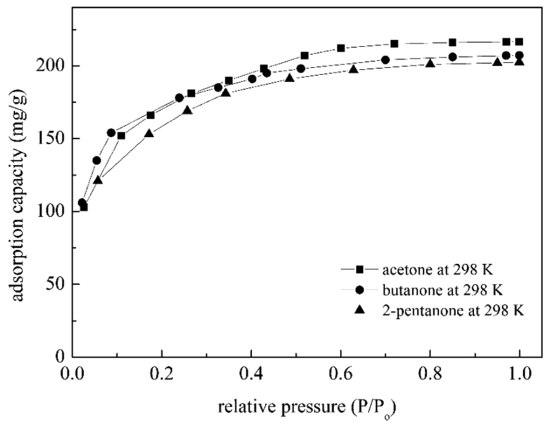

Figure 6. Adsorption capacities for ketones. Standard uncertainties are $u(T)$ = 0.1 K and $u(P)$ = 0.026 kPa and the mean standard uncertainties are acetone = 1.66, butanone = 0.91, and 2-pentanone = 1.53.

adsorption capacity is consistent with the polarity at lower pressures. This result was attributed to the dipole−dipole interaction between polar adsorbates, which dominated the adsorption. Since the polarities decrease in the order of butanone, acetone, and 2-pentanone, the attractions between molecules were also in the same order. Therefore, the trend of the adsorption capacity for adsorptions of ketones by the activated carbon is consistent with the molecular attraction at lower pressures.

Figure 6 also shows that at higher pressures, the adsorption capacities decreased in the order of acetone, butanone, and 2-pentanone. Since the molecular size of acetone is smaller than

https://dx.doi.org/10.1021/acsomega.0c06260
ACS Omega 2021, 6, 5825−5835

that of butanone, the filling effect of acetone is greater than that of butanone at higher pressures. The dipole−dipole interaction dominating the adsorption at lower pressures could translate into the filling effect dominating the adsorption at higher pressures. Therefore, at higher pressures, the adsorption capacity of activated carbon is larger for acetone than for butanone and 2-pentanone.

3.5. Effect of the Operating Temperature on the Adsorption Capacity. In general, the adsorption capacity is affected by the operating temperature. VOCs were adsorbed by activated carbon at controlled temperatures to acquire adsorption isotherms, thereby examining how the adsorption capacity is affected by the operating temperature, and also to obtain a more suitable adsorption isotherm model from fitting the equilibrium data. Figures 7−15 show the adsorption isotherms for VOCs at temperatures of 288−313 K. The results demonstrate that the adsorption capacities for all VOCs decreased with increases in the operating temperature. Since the adsorption of VOCs by activated carbon is an exothermic reaction, the adsorption amount decreased naturally with increases in the temperature.

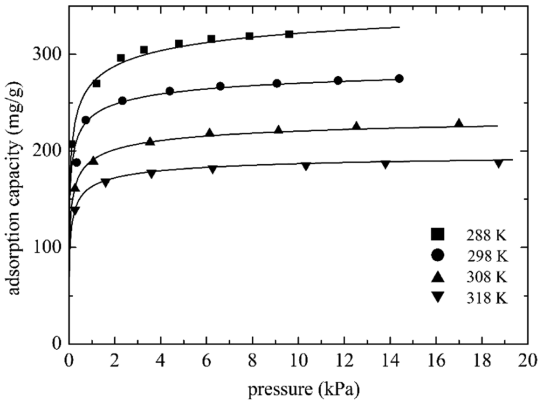

Figure 7. Adsorption isotherms for *n*-hexane adsorption by activated carbon at a controlled temperature. Standard uncertainties are $u(T)$ = 0.1 K and $u(P)$ = 0.026 kPa and the mean standard uncertainties are 1.06 at 288 K, 1.13 at 298 K, 1.42 at 308 K, and 1.44 at 318 K.

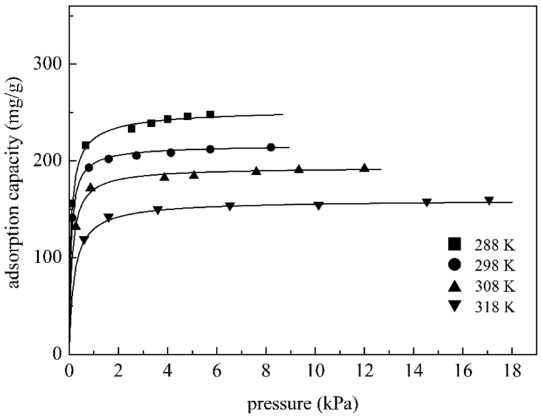

Figure 8. Adsorption isotherms for cyclohexane adsorption by activated carbon at a controlled temperature. Standard uncertainties are $u(T)$ = 0.1 K and $u(P)$ = 0.026 kPa and the mean standard uncertainties are 1.06 at 288 K, 0.97 at 298 K, 0.95 at 308 K, and 0.87 at 318 K.

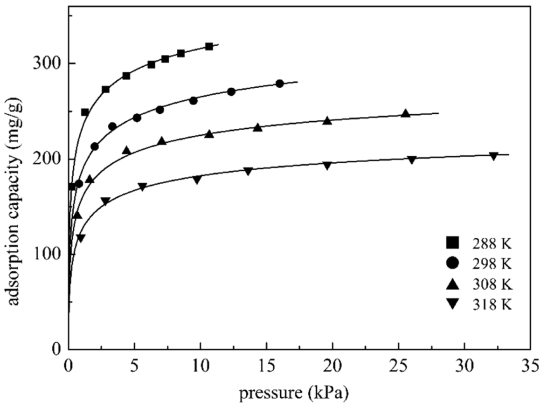

Figure 9. Adsorption isotherms for 1-hexene adsorption by activated carbon at a controlled temperature. Standard uncertainties are $u(T)$ = 0.1 K and $u(P)$ = 0.026 kPa and the mean standard uncertainties are 1.11 at 288 K, 1.37 at 298 K, 1.07 at 308 K, and 0.93 at 318 K.

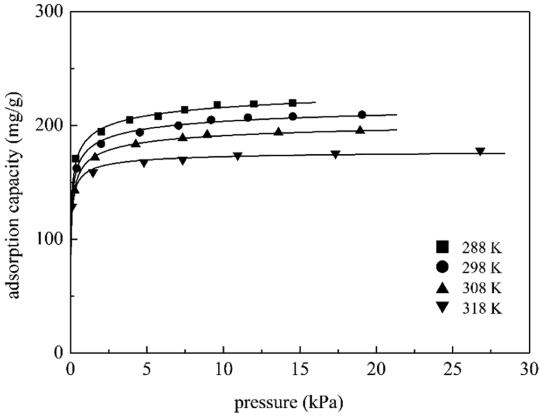

Figure 10. Adsorption isotherms for 2-methylpentane adsorption by activated carbon at a controlled temperature. Standard uncertainties are $u(T)$ = 0.1 K and $u(P)$ = 0.026 kPa and the mean standard uncertainties are 1.07 at 288 K, 1.56 at 298 K, 1.10 at 308 K, and 1.12 at 312 K.

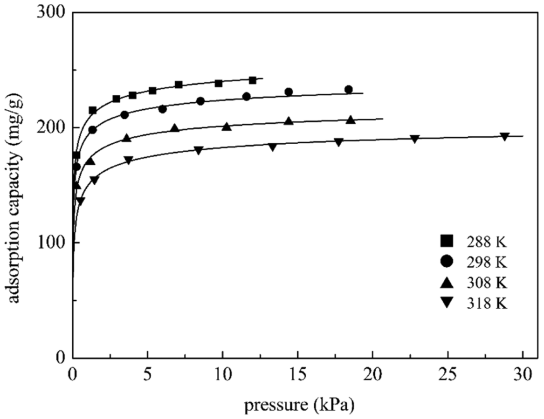

Figure 11. Adsorption isotherms for 3-methylpentane adsorption by activated carbon at a controlled temperature. Standard uncertainties are $u(T)$ = 0.1 K and $u(P)$ = 0.026 kPa and the mean standard uncertainties are 1.21 at 288 K, 1.40 at 298 K, 1.34 at 308 K, and 0.95 at 312 K.

3.6. Discussions on the Regression of Adsorption Isotherms. The Toth adsorption isotherm model is suitable for modeling heterogeneous adsorption, such as a gaseous

https://dx.doi.org/10.1021/acsomega.0c06260
ACS Omega 2021, 6, 5825−5835

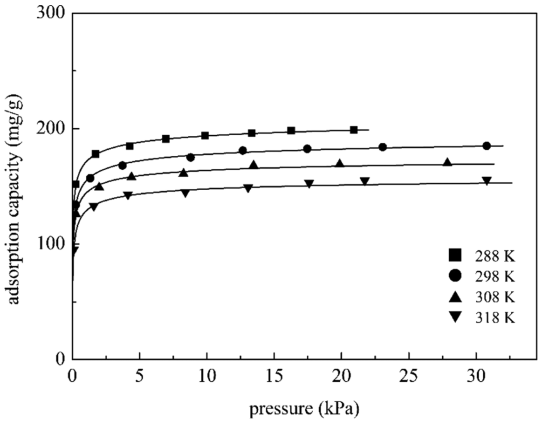

Figure 12. Adsorption isotherms for 2,2-dimethylbutane adsorption by activated carbon at a controlled temperature. Standard uncertainties are $u(T)$ = 0.1 K and $u(P)$ = 0.026 kPa and the mean standard uncertainties are 1.52 at 288 K, 1.58 at 298 K, 1.26 at 308 K, and 0.93 at 312 K.

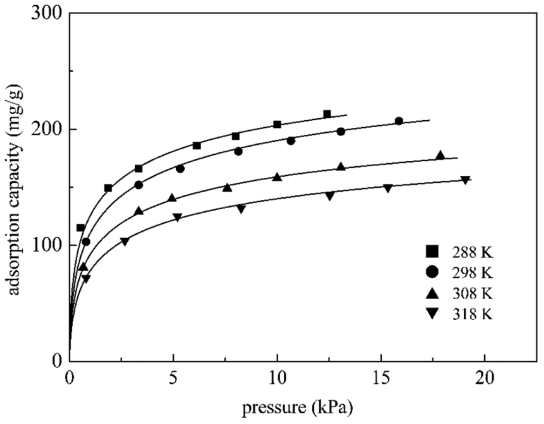

Figure 13. Adsorption isotherms for acetone adsorption by activated carbon at a controlled temperature. Standard uncertainties are $u(T)$ = 0.1 K and $u(P)$ = 0.026 kPa and the mean standard uncertainties are 1.62 at 288 K, 1.66 at 298 K, 1.47 at 308 K, and 1.05 at 312 K.

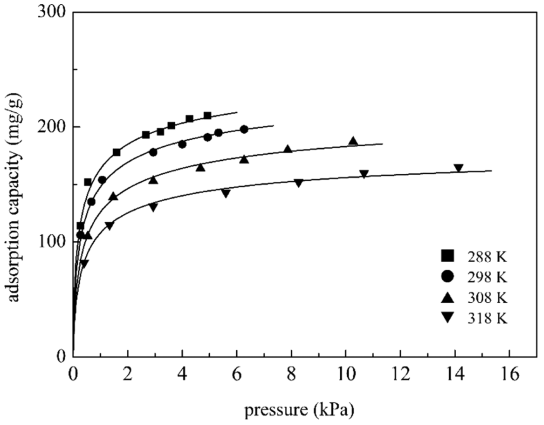

Figure 14. Adsorption isotherms for butanone adsorption by activated carbon at a controlled temperature. Standard uncertainties are $u(T)$ = 0.1 K and $u(P)$ = 0.026 kPa and the mean standard uncertainties are 1.16 at 288 K, 0.91 at 298 K, 1.10 at 308 K, and 1.12 at 312 K.

adsorbate adsorbed by a solid adsorbent, and the Langmuir adsorption model and Henry's law were merged into this

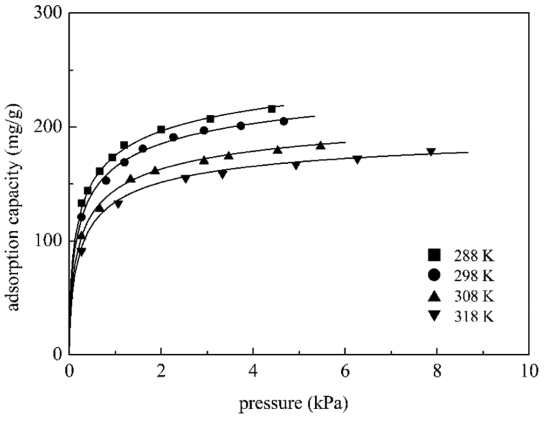

Figure 15. Adsorption isotherms for 2-pentanone adsorption by activated carbon at a controlled temperature. Standard uncertainties are $u(T)$ = 0.1 K and $u(P)$ = 0.026 kPa and the mean standard uncertainties are 1.43 at 288 K, 1.53 at 298 K, 1.55 at 308 K, and 1.11 at 312 K.

model. Therefore, the Toth adsorption isotherm model was used to fit the experimental data in this study. The adsorption data for VOCs adsorbed by the activated carbon were fitted in the software Systat 10.0, and the constants were determined by convergent regression. The Toth adsorption isotherm model can be formulated as follows

$$q = q^{\exp}\frac{KP}{[1 + KP^t]^{1/t}} \quad (1)$$

$$K = K_0 \exp\left[\frac{-\Delta H_{ads}}{RT_0}\left(\frac{T_0}{T} - 1\right)\right] \quad (2)$$

where in eq 1, q is the equilibrium adsorption capacity for an adsorbent (mg/g), $q^{\exp}$ is the adsorption capacity under an equilibrium state (mg/g), K is the adsorption equilibrium constant (kPa^{-1}), P is gas pressure, and t can be regarded as a parameter describing the degree of heterogeneity of the adsorption system. In eq 2, T_0 is the lowest temperature among the operating temperatures (K), T is the operating temperature (K), R is the ideal gas constant (J/(mol K)), K_0 is the adsorption equilibrium constant (kPa^{-1}) at temperature T_0, and ΔH_{ads} is the enthalpy of adsorption (J/mol). These values obtained from the Toth adsorption model and fitted by the adsorption data are summarized in Table 5. The adsorption equilibrium constants for all VOCs decreased with increases in temperature because such increases are unfavorable for adsorption. In addition, the adsorption equilibrium constant is a function of temperature; therefore, it decreases with increases in temperature, as shown in eq 2.

The parameter t is usually used to indicate the degree of heterogeneity of a catalytic reaction system. As mentioned above, t described the degree of the system used in this study. When the value of t deviates from 1, the degree of heterogeneity is more significant. When t approaches 1, the Toth adsorption isotherm model can be simplified to the Langmuir adsorption isotherm model, indicating a higher homogeneity for the adsorption system. Since the gaseous VOCs were adsorbed by the solid activated carbon, the nature of the adsorbent−adsorbate pair was closer to that of a heterogeneous system. All of the values of t were smaller than 1, as shown in Table 5, revealing that all of the adsorption runs were heterogeneous. The values of t increased with increases in

https://dx.doi.org/10.1021/acsomega.0c06260
ACS Omega 2021, 6, 5825−5835

Table 5. Parameters, Standard Uncertainties (D), and Values of R^2 for the Toth Adsorption Isotherm Model Fitted by the Adsorption Data[a]

adsorbate	T (K)	q^{sat} (mg/g)	K (kPa^{-1})	t	D	R^2
n-hexane	288	393	269.08	0.286	1.06	0.992
	298	304	139.81	0.344	1.13	0.997
	308	248	66.43	0.367	1.42	0.996
	318	204	34.40	0.418	1.44	0.997
cyclohexane	288	256	3.72	0.690	1.06	0.993
	298	217	2.40	0.856	0.97	0.994
	308	194	1.46	0.883	0.95	0.990
	318	161	0.61	0.930	0.83	0.994
1-hexene	288	451	23.12	0.295	1.11	0.997
	298	394	13.23	0.301	1.37	0.995
	308	321	8.49	0.325	1.07	0.996
	318	260	5.19	0.343	0.93	0.998
2-methylpentane	288	251	303.69	0.305	1.07	0.995
	298	231	143.12	0.338	1.56	0.992
	308	212	65.49	0.379	1.10	0.999
	318	180	30.48	0.500	1.12	0.993
3-methylpentane	288	282	359.50	0.296	1.21	0.997
	298	257	161.10	0.327	1.40	0.996
	308	231	71.70	0.350	1.34	0.995
	318	215	30.05	0.363	0.95	0.997
2,2-dimethylbutane	288	218	296.77	0.324	1.52	0.997
	298	201	127.69	0.343	1.58	0.999
	308	180	64.28	0.388	1.26	0.998
	318	162	35.30	0.412	0.93	0.996
acetone	288	338	2.63	0.325	1.26	0.993
	298	329	1.69	0.333	1.66	0.997
	308	275	1.35	0.342	1.47	0.997
	318	251	0.99	0.347	1.05	0.998
butanone	288	270	2.94	0.447	1.16	0.993
	298	253	2.11	0.461	0.91	0.998
	308	226	1.50	0.476	1.10	0.992
	318	190	1.27	0.498	1.12	0.993
2-pentanone	288	291	5.01	0.406	1.43	0.996
	298	271	4.00	0.425	1.53	0.994
	308	230	2.91	0.458	1.55	0.995
	318	207	1.91	0.518	1.11	0.994

[a]Standard uncertainties are $u(T)$ = 0.1 K and $u(P)$ = 0.026 kPa and standard uncertainties for the fitted model are given in the table.

temperature, gradually approaching 1. As shown in Figures 7−15, at high temperatures, the resemblance to the Langmuir model was greater. Therefore, the value of t increased and approached 1 with increases in temperature. The degree of agreement between the experimental data and the adsorption isotherm model was investigated by fitting the adsorption isotherm model with the experimental data. The deviation between the experimental data and the theoretical values calculated from the fitted adsorption isotherm is expressed by the mean deviation D, and its formula is shown as follows

$$D = \frac{1}{N}\sum_{i=1}^{n}\left|\frac{q_i^{exp} - q_i^{th}}{q_i^{exp}}\right| \quad (3)$$

where D is the mean deviation, N is the number of experimental runs, q_i^{exp} is the experimental adsorption capacity (mg/g), and q_i^{th} is the adsorption capacity (mg/g) calculated from the fitted adsorption isotherm model. All of the mean deviations approached zero, as shown in Table 5, indicating that the adsorption capacities measured from experimental runs and the theoretical values calculated from the fitted Toth adsorption isotherm model were consistent with each other. In addition, all of the coefficients of determination, R^2, were larger than 0.99. The Toth adsorption isotherm model fitted well the adsorption capacities in this study, as demonstrated by the mean deviation and the coefficient of determination.

4. CONCLUSIONS

Gravimetric adsorption equipment with a microbalance was used in this study. Activated carbon was used as an adsorbent for nine VOCs (*n*-hexane, cyclohexane, 1-hexene, 2-methylpentane, 3-methylpentane, 2,2-dimethylbutane, acetone, butanone, and 2-pentanone) in the adsorption system. The adsorption experiments were performed to obtain adsorption isotherms, and then the adsorption data were used to fit the Toth adsorption isotherm model to obtain the parameters in the Toth adsorption isotherm model. The experimental results showed that the geometric structure dominated the adsorption of nonpolar and weak polar VOCs by activated carbon. The adsorption performance was affected by the adsorbate−adsorbent and the adsorbate−adsorbate interactions, and these interactions could be influenced by the change in pressure. At lower pressures, the adsorption capacity was larger for *n*-hexane than for 1-hexene, but at higher pressures, the opposite was true due to the larger dipole−dipole interaction for 1-hexene. The factors that affected the adsorption of ketones by the activated carbon were polarity and the geometric structure. The adsorption capacities were dominated by the polarity of the adsorbate at lower pressures and by the geometric structure at higher pressures. All of the adsorption isotherms in this study were type 1 due to the excellent affinity between VOCs and the nanoscale activated carbon, especially for alkanes and alkenes. Finally, the Toth adsorption isotherm model was fitted by the experimental data, and the values of R^2 were larger than 0.99. The results demonstrated that the experimental data and the Toth adsorption isotherm model were consistent with each other.

AUTHOR INFORMATION

Corresponding Author

Hung-Ta Wu − *Department of Chemical and Materials Engineering, National Ilan University, Yilan City, Taiwan 260, ROC*; orcid.org/0000-0002-0794-4536; Email: htwu@niu.edu.tw

Authors

Show-Chu Huang − *Department of Chemical Engineering, Chung Yuan Christian University, Taoyuan City 32023, Taiwan, ROC*

Tsair-Wang Chung − *Department of Chemical Engineering, Chung Yuan Christian University, Taoyuan City 32023, Taiwan, ROC*

Complete contact information is available at: https://pubs.acs.org/10.1021/acsomega.0c06260

Notes

The authors declare no competing financial interest.

https://dx.doi.org/10.1021/acsomega.0c06260
ACS Omega 2021, 6, 5825−5835

■ ACKNOWLEDGMENTS

The authors are thankful to all memberships of the separation technology laboratory, Department of Chemical Engineering, Chung Yuan Christian University, for help with completing this research.

■ REFERENCES

(1) Widiana, D. R.; Wang, Y. F.; You, S. J.; Yang, H. H.; Wang, L. C.; Tsai, J. H.; Chen, H. M. Air Pollution Profiles and Health Risk Assessment of Ambient Volatile Organic Compounds above a Municipal Wastewater Treatment Plant, Taiwan. *Aerosol Air Qual. Res.* **2019**, *19*, 375−382.

(2) Khan, F. I.; Ghoshal, A. K. Removal of Volatile Organic Compounds from polluted air. *J. Loss Prev. Process Ind.* **2000**, *13*, 527−545.

(3) Huang, C. C. Polyneuropathy Induced by n-Hexane Intoxication in Taiwan. *Acta Neurol. Taiwan.* **2008**, *17*, 3−10.

(4) Pegas, P. N.; Evtyugina, M. G.; Alves, C. A.; Nunes, T.; Cerqueira, M.; Franchi, M.; Pio, C.; Almeida, S. M.; Freitas, M. C. Outdoor/Indoor Air Quality in Primary Schools in Lisbon: a Preliminary Study. *Quim. Nova* **2010**, *33*, 1145−1149.

(5) Nawaz, Z.; Tang, X.; Wei, F. Hexene Catalytic Cracking over 30% SAPO-34 Catalyst for Propylene Maximization: Influence of Reaction Conditions and Reaction Pathway Exploration. *Braz. J. Chem. Eng.* **2009**, *26*, 705−712.

(6) Rösch, C.; Kohajda, T.; Röder, S.; Bergen, M.; Schlink, U. Relationship between Sources and Patterns of VOCs in Indoor Air. *Atoms. Pollut. Res.* **2014**, *5*, 129−137.

(7) Norbäck, D.; Hashim, J. H.; Hashim, Z.; Ali, F. Volatile Organic Compounds (VOC), Formaldehyde and Nitrogen Dioxide (NO_2) in Schools in Johor Bahru, Malaysia: Associations with Rhinitis, Ocular, Throat and Dermal Symptoms, Headache and Fatigue. *Sci. Total Environ.* **2017**, *592*, 153−160.

(8) Gallego, E.; Roca, X.; Perales, J. F.; Guardino, X. Determining Indoor Air Quality and Identifying the Origin of Odour Episodes in Indoor Environments. *J. Environ. Sci.* **2009**, *21*, 333−339.

(9) Araizaga, A. E.; Mancilla, Y.; Mendoza, A. Volatile Organic Compound Emissions from Light-Duty Vehicles in Monterrey, Mexico: a Tunnel Study. *Int. J. Environ. Res.* **2013**, *7*, 277−292.

(10) Schuring, D.; Koriabkina, A. O.; Jong, A. M.; Smit, B.; Santen, R. A. Adsorption and Diffusion of n-Hexane/2-Methylpentane Mixtures in Zeolite Silicalite: Experiments and Modeling. *J. Phys. Chem. B* **2001**, *105*, 7690−7698.

(11) Graham, L. A.; Noseworthy, L.; Fugler, D.; O'Leary, K.; Karman, D.; Grande, C. Contribution of Vehicle Emissions from an Attached Garage to Residential Indoor Air Pollution Levels. *J. Air Waste Manage. Assoc.* **2004**, *54*, 563−584.

(12) Han, S. W.; Lee, J. H.; Kim, J. S.; Oh, S. H.; Park, Y. K.; Kim, H. Gaseous by-products from the TiO_2 Photocatalytic Oxidation of Benzene. *Environ. Eng. Res.* **2008**, *13*, 14−18.

(13) Akihama, K.; Takatori, Y.; Nakakita, K. Effect of Hydrocarbon Molecular Structure on Diesel Exhaust Emissions. *R&D Rev. Toyota CRDL* **2002**, *37*, 46−52.

(14) Liu, C.; Zhang, C.; Mu, Y.; Liu, J.; Zhang, Y. Emission of Volatile Organic Compounds from Domestic Coal Stove with the Actual Alternation of Flaming and Smoldering Combustion Processes. *Environ. Pollut.* **2017**, *221*, 385−391.

(15) Garland, M.; Baiker, A.; Wokaun, A. Alumina-Supported Platinum-Rhenium Dehydrogenation Catalysts: Influence of Metal Ratio and Precursors on Catalytic Behavior. *Ind. Eng. Chem. Res.* **1991**, *30*, 440−447.

(16) Vogelzang, M. W.; Ponec, V. Reactions of 2,2-Dimethylbutane on Iridium: the Role of Surface Carbonaceous Layers and Metal Particle Size. *J. Catal.* **1988**, *111*, 77−87.

(17) Lemaire, E.; Decrette, A.; Bellat, J. P.; Simon, J. M.; Méthivier, A.; Jolimaître, E. Adsorption and Diffusion of Linear and Dibranched C6 Paraffins in a ZSM-5 Zeolite. *Stud. Surf. Sci. Catal.* **2002**, *142*, 1571−1578.

(18) Ferreira, A. F. P.; Mittelmeijer-Hazeleger, M. C.; Granato, M. A.; Martins, V. F. D.; Rodrigues, A. E.; Rothenberg, G. Sieving Di-branched from Mono-branched and Linear Alkanes Using ZIF-8: Experimental Proof and Theoretical Explanation. *Phys. Chem. Chem. Phys.* **2013**, *15*, 8795−8804.

(19) Mofidi, A.; Asilian, H.; Jafari, A. J. Adsorption of Volatile Organic Compounds on Fluidized Activated Carbon Bed. *Health Scope* **2013**, *2*, 84−89.

(20) Dehdashti, A.; Khavanin, A.; Rezaee, A.; Assilian, H.; Motalebi, M. Application of Microwave Irradiation for the Treatment of Adsorbed Volatile Organic Compounds on Granular Ranular Activated Carbon. *Iran. J. Environ. Health. Sci. Eng.* **2011**, *8*, 85−94.

(21) Pak, S. H.; Jeon, Y. W. Effect of Vacuum Regeneration of Activated Carbon on Volatile Organic Compound Adsorption. *Environ. Eng. Res.* **2017**, *22*, 169−174.

(22) Sullivan, P. D.; Rood, M. J.; Dombrowski, K. D.; Hay, K. J.; M.ASCE. Capture of Organic Vapors Using Adsorption and Electrothermal Regeneration. *J. Environ. Eng.* **2004**, *130*, 258−267.

(23) Lemus, J.; Martin-Martinez, M.; Palomar, J.; Gomez-Sainero, L.; Gilarranz, M. A.; Rodriguez, J. J. Removal of Chlorinated Organic Volatile Compounds by Gas Phase Adsorption with Activated Carbon. *Chem. Eng. J.* **2012**, *211−212*, 246−254.

(24) Kalender, M.; Akosman, C. Removal of Chlorinated Volatile Organic Compounds by Fixed Bed Adsorption Technique: Adsorption Equilibrium and Breakthrough Analyses. *Rom. Biotech. Lett.* **2015**, *20*, 10245−10256.

(25) Das, D.; Gaur, V.; Verma, N. Removal of Volatile Organic Compound by Activated Carbon Fiber. *Carbon* **2004**, *42*, 2949−2962.

(26) Gupta, V. K.; Verma, N. Removal of Volatile Organic Compounds by Cryogenic Condensation Followed by Adsorption. *Chem. Eng. Sci.* **2002**, *57*, 2679−2696.

(27) Tefera, D. T.; Hashisho, Z.; Philips, J. H.; Anderson, J. E.; Nichols, M. Modeling Competitive Adsorption of Mixtures of Volatile Organic Compounds in a Fixed-Bed of Beaded Activated Carbon. *Environ. Sci. Technol.* **2014**, *48*, 5108−5117.

(28) Cabrera-Codony, A.; Santos-Clotas, E.; Ania, C. O.; Martín, M. J. Competitive Siloxane Adsorption in Multicomponent Gas Streams for Biogas Upgrading. *Chem. Eng. J.* **2018**, *344*, 565−573.

(29) Ma, C.; Wang, X.; Wang, X.; Yuan, B.; Wu, Y.; Li, Z. Novel Glucose-Based Adsorbents (Glc-As) with Preferential Adsorption of Ethane over Ethylene and High Capacity. *Chem. Eng. Sci.* **2017**, *172*, 612−621.

(30) Chang, S. J.; Wi, S.; Jeong, S. G.; Kim, S. Evaluation of the Adsorption Performance and Sustainability of Exfoliated Graphite Nanoplatelets (xGnP) for VOCs. *Materials* **2015**, *8*, 7615−7621.

(31) Moon, H. S.; Kim, I. S.; Kang, S. J.; Ryu, S. K. Adsorption of Volatile Organic Compounds Using Activated Carbon Fiber Filter in the Automobiles. *Carbon Lett.* **2014**, *15*, 203−209.

(32) De Yuso, A. M.; Izquierdo, M. T.; Rubio, B.; Carrott, P. J. M. Adsorption of Toluene and Toluene-water Vapor Mixture on Almond Shell Based Activated Carbons. *Adsorption* **2013**, *19*, 1137−1148.

(33) Anuradha, S.; Raj, K.; Joseph, A.; Elangovan, T.; Viswanathan, B. Adsorption of VOC on Steam Activated Carbon Derived from Coconut Shell Charcoal. *Indian J. Chem. Technol.* **2014**, *21*, 345−349.

(34) Pourfayaz, F.; Boroun, S.; Babaei, J.; Hoseinzadeh, B. E. An Evaluation of the Adsorption Potential of MWCNTs for Benzene and Toluene Removal. *Int. J. Nanosci. Nanotechnol.* **2014**, *10*, 27−34.

(35) Aziz, A.; Kim, M.; Kim, S.; Kim, K. S. Adsorption and Kinetic Studies of Volatile Organic Compounds (VOCs) on Seed Assisted Template Free ZSM-5 Zeolite in Air. *J. Nano. Adv. Mater.* **2017**, *5*, 1−9.

(36) Wang, Y. F.; Peng, C. F.; Chao, H. P. Sorption of Volatile Organic Compounds on Organic Substance-Modified Titanate Nanotubes. *Aerosol Air Qual. Res.* **2015**, *15*, 2688−2699.

(37) Aghababaei, N. Removal of Acetone Volatile Organic Compound Using Modified Clinoptilolite Natural Zeolite of Iran. *Bulg. Chem. Commun.* **2016**, *48*, 16−20.

https://dx.doi.org/10.1021/acsomega.0c06260
ACS Omega 2021, 6, 5825−5835

(38) Nwali, C. J. Volatile Organic Compounds Removal by Adsorption on Activated Carbon Filters. *Int. J. Adv. Res. Chem. Sci.* **2014**, *1*, 38−43.
(39) Reid, R. C.; Prausnitz, J. M.; Sherwood, T. K. *The Properties of Gases and Liquids*, 3rd ed.; McGraw-Hill, 1977.
(40) Cavalcante, C. L.; Ruthven, D. M., Jr. Adsorption of Branched and Cyclic Paraffins in Silicalite. 1. Equilibrium. *Ind. Eng. Chem. Res.* **1995**, *34*, 177−184.
(41) Prausnitz, J. M.; Lichtenthaler, R. N.; Azevedo, E. G. *Molecular Thermodynamics of Fluid-Phase Equilibria*, 3rd ed.; Prentice Hall, 1999.
(42) Perry, R. H.; Green, D. W.; Maloney, J. O. *Perry's Chemical Engineers' Handbook*, 7th ed.; McGraw-Hill, 1997.
(43) Zhao, X. S.; Ma, Q.; Lu, G. Q. VOC Removal: Comparison of MCM-41 with Hydrophobic Zeolites and Activated Carbon. *Energy Fuels* **1998**, *12*, 1051−1054.
(44) Ramirez, D.; Sullivan, P. D.; Rood, M. J.; Hay, K. J.; M.ASCE. Equilibrium Adsorption of Phenol-, Tire-, and Coal-Derived Activated Carbons for Organic Vapors. *J. Environ. Eng.* **2004**, *130*, 231−241.
(45) Zhu, W.; Groen, J. C.; Miltenburg, A.; Kapteijn, F.; Moulijn, J. A. Comparison of Adsorption Behaviour of Light Alkanes and Alkenes on Kureha Activated Carbon. *Carbon* **2005**, *43*, 1416−1423.
(46) Zhu, W.; Kapteijn, F.; Moulijn, J. A. Shape Selectivity in the Adsorption of Propane/Propene on the All-Silica DD3R. *Chem. Commun.* **1999**, *24*, 2453−2454.
(47) Zhu, W.; Kapteijn, F.; Moulijn, J. A.; Exter, M. C.; Jansen, J. C. Shape Selectivity in Adsorption on the All-Silica DD3R. *Langmuir* **2000**, *16*, 3322−3329.
(48) Olson, D. H.; Camblor, M. A.; Villaescusa, L. A.; Kuehl, G. H. Light Hydrocarbon Sorption Properties of Pure Silica Si-CHA and ITQ-3 and High Silica ZSM-58. *Microporous Mesoporous Mater.* **2004**, *67*, 27−33.
(49) Smoot, L. D.; Pratt, D. T. *Pulverized-Coal Combustion and Gasification: Theory and Applications for Continuous Flow Processes*; Springer, 1979.
(50) Dyson, N.; Littlewood, A. B. Effect of Organic Vapour Molecules on the Viscosities of Hydrogen and Helium. *Trans. Faraday Soc.* **1967**, *63*, 1895−1905.
(51) van Leeuwen, M. E. Derivation of Stockmayer potential parameters for polar fluids. *Fluid Phase Equilib.* **1994**, *99*, 1−18.
(52) Jiménez-Cruz, F.; Laredo, G. C. Molecular size evaluation of linear and branched paraffins from the gasoline pool by DFT quantum chemical calculations. *Fuel* **2004**, *83*, 2183−2188.
(53) Albrecht, E.; Baum, G.; Bellunato, T.; Bressan, A.; Torre, S. D.; D'Ambrosio, C.; Davenport, M.; Dragicevic, M.; Pinto, S. D.; Fauland, P.; Ilie, S.; Lenzen, G.; Pagano, P.; Piedigrossi, D.; Tessarotto, F.; Ullaland, O. VUV absorbing vapours in n-perfluorocarbons. *Nucl. Instrum. Methods Phys. Res., Sect. A* **2003**, *510*, 262−272.
(54) Lashaki, M. J.; Fayaz, M.; Niknaddaf, S.; Hashisho, Z. Effect of the adsorbate kinetic diameter on the accuracy of the Dubinin−Radushkevich equation for modeling adsorption of organic vapors on activated carbon. *J. Hazard. Mater.* **2012**, *241*−*242*, 154−163.
(55) Sochard, S.; Fernandes, N.; Reneaume, J. M. Modeling of adsorption isotherm of a binary mixture with real adsorbed solution theory and nonrandom two-liquid model. *AIChE J.* **2010**, *56*, 3109−3119.
(56) Yonli, A. H.; Gener-Batonneau, I.; Mignard, S. Single and competitive adsorption of linear and branched paraffins over silicalite: thermodynamic and kinetic Study. *Am. Chem. Sci. J.* **2015**, *5*, 70−78.

https://dx.doi.org/10.1021/acsomega.0c06260
ACS Omega 2021, 6, 5825−5835